Large spin, magnetically anisotropic, octametallic vanadium(III) clusters with strong ferromagnetic coupling†

Rachel Shaw,[a] Floriana Tuna,[a] Wolfgang Wernsdorfer,[b] Anne-Laure Barra,[c] David Collison*[a] and Eric J. L. McInnes*[a]

Received (in Cambridge, UK) 13th July 2007, Accepted 20th September 2007
First published as an Advance Article on the web 5th October 2007
DOI: 10.1039/b710732c

Syntheses, structural and magnetic and EPR data are reported for two octametallic V^{III} clusters with anisotropic $S = 4$ ground states arising from strong ferromagnetic exchange interactions.

Molecules with anisotropic, large ground state electronic spins (S) are of interest for their fundamental physics, including magnetic bistability and quantum tunnelling of magnetisation effects. Bistability in these "single molecule magnets" (SMMs)[1] requires large $|D|S^2$, where D is the axial zero-field splitting (ZFS) giving rise to the magnetic anisotropy. A further desirable property is that the ground state is well isolated to prevent relaxation *via* excited S states – this requires strong magnetic exchange interactions $|J|$. Most known SMMs contain $Mn^{III/IV}$ or Fe^{III}.[1] An attractive alternative is the $S = 1$, V^{III} ion because of its typically very large $|D|$.[2] Furthermore, some V^{III} dimers show extraordinarily strong ferromagnetic exchange,[3] for example $J > +200$ cm^{-1} in $[(Me_3tacn)_2V_2O(O_2CPh)_2]I_2$. Although we have recently been successful in preparing high nuclearity V^{III} and $V^{III/IV}$ clusters *via* solvothermal methods,[4,5] there are still very few large V^{III} clusters known,[4–6] and only one V^{III}-based SMM (assigned on the basis of ac susceptibility measurements).[7] Here we report a family of octametallic V^{III} clusters from reaction of 1,2,3-triazoles with $[V_2Cl_9]^{3-}$, surprisingly not previously exploited as a starting material for V^{III} cluster chemistry. These $\{V^{III}_8\}$ complexes exhibit very strong ferromagnetic $V^{III}\cdots V^{III}$ coupling ($J > +100$ cm^{-1}), previously only seen in bimetallics, giving anisotropic $S = 4$ ground states, the largest known for a vanadium-based cluster.

$[N^nBu_4]_3[V_2Cl_9]$ was prepared by an adaptation of Christou's method,[8] from $[VCl_3(THF)_3]$ (0.81 mmol) and $[N^nBu_4]Cl$ (1.22 mmol) in CH_2Cl_2 (9 ml) at room temperature. Solvothermal reaction of $[N^nBu_4]_3[V_2Cl_9]$ (0.40 mmol) in THF (9 ml) with btaH (0.81 mmol; btaH = benzotriazole) and Me_3CCO_2H (0.40 mmol) at 150 °C under an inert atmosphere gives large dark brown crystals of $[N^nBu_4]_2[V_8O_4(bta)_8(O_2CCMe_3)_4Cl_6]$ **1** (Fig. 1) directly on slow cooling and in excellent yield (70%).‡ **1** can also be isolated from reaction with $Na(O_2CCMe_3)$ but is accompanied by an insoluble byproduct.

1·4THF crystallises in the space group $P2_1/n$, and the dianion lies on an inversion centre.§ Its inorganic core is composed of two fragments common in cluster chemistry. The central four vanadium ions V1,1A,4,4A define a planar "butterfly" where V1,1A and V4,4A are the body and wingtip ions, respectively, bridged by O1 and O1A. The $\{V_4(\mu_3\text{-}O)_2\}^{8+}$ butterfly vertex-shares (*via* V1,1A) with two planar $\{V_3(\mu_3\text{-}O)\}^{7+}$ oxo-centred (O2) triangles defined by the peripheral vanadium ions (V1-3, V1A-3A), thus forming an overall $\{V_8O_4\}^{16+}$ core. The planes of the triangles lie at 90° to the plane of the butterfly. The cluster is bound by eight μ_3-bta$^-$ ligands, linking V4(A) to V2(A) or V3(A) centred on V1(A). The outer edge of the two V_3 triangles (V2···V3) are bridged by two μ_2-carboxylates. A terminal chloride completes the pseudo-octahedral coordination geometry at each of V2–4 and symmetry equivalents. V1 and V1A have $\{VN_4O_3\}$ coordination spheres and thus are rare examples of seven-coordinate V^{III} ions

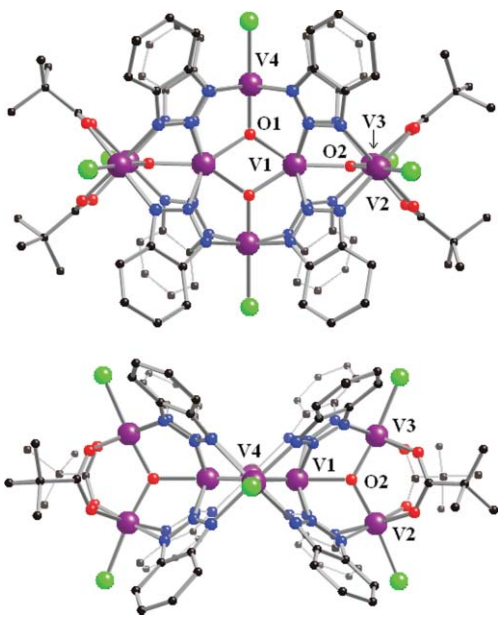

Fig. 1 Structure of the dianion of **1**, viewed perpendicular to the planar central $\{V_4\}$ butterfly (top) and to the peripheral $\{V_3\}$ triangles (bottom). Selected metric parameters: V–O1,2 1.799(3)–2.024(3), other V–O 2.005(3)–2.017(3), V–N 2.117(3)–2.160(3), V–Cl 2.3494(12)–2.3615(12) Å; V–O1,2–V 111.84(12)–124.36(14)°. Scheme: V (purple), O (red), N (blue), Cl (green), C (black); H omitted for clarity.

[a]*School of Chemistry, The University of Manchester, Manchester, UK M13 9PL. E-mail: david.collison@manchester.ac.uk; eric.mcinnes@manchester.ac.uk; Fax: +44 (0)161-275-4616; Tel: +44-161-275-4469*
[b]*Laboratoire Louis Néel-CNRS, 38042, Grenoble, Cedex 9, France*
[c]*LCMI-CNRS, 38042, Grenoble, Cedex 9, France*

† Electronic supplementary information (ESI) available: Fig. S1: View of the structure of the dianion of **2**. Fig. S2: χT *vs.* T for **2** measured in 1 T applied magnetic field. Fig. S3: 190 GHz EPR spectrum at 5 K of a loose polycrystalline sample of **1**. Fig. S4: 230 GHz EPR spectrum at 5 K of a polycrystalline sample of **1** restrained in eicosane wax. Fig. S5: Low-temperature M *vs.* H loops for a single crystal of **1**. Table S1: Bond valence sum calculations for the vanadium ions in **1** and **2**. See DOI: 10.1039/b710732c

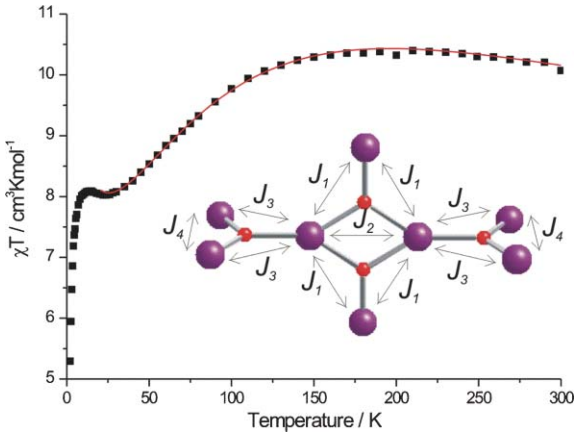

Fig. 2 χT *vs.* T for **1** measured in 1 T applied magnetic field (black squares) and best fit to 20 K (red line) using the coupling scheme in the insert and the spin-Hamiltonian and parameters in the text.

(capped trigonal prismatic). All eight vanadium ions are in the +3 oxidation state, as required by charge balance and supported by bond valence sum calculations (see ESI†) and consistent with magnetic measurements (see below).

The synthetic route to **1** is versatile and a family of $[N^nBu_4]_2$-$[V_8O_4(5,6\text{-}R_2\text{-bta})_8(O_2CR')_4Cl_6]$ compounds can be obtained with, for example, R = H, Me; R′ = Me, Et, CF_3, CMe_3, CPh_3, Ph, *o*-PhC_6H_4 (*e.g.*, see Fig. S1, ESI,† for R = H, R′ = Ph derivative, compound **2**).§

χT (χ = molar magnetic susceptibility) for **1** at 300 K is 10.1 cm^3 K mol^{-1}, significantly greater than expected for eight uncoupled V^{III} ions, increasing on cooling to a broad maximum at 150–200 K (Fig. 2).¶ This implies significant ferromagnetic interactions. On further cooling χT drops to a crude plateau at *ca.* 8.0 cm^3 K mol^{-1} between 25 and 15 K indicating the action of antiferromagnetic interactions. Below 15 K χT collapses due to ZFS (see below). We have fit these data down to 20 K using the exchange Hamiltonian (1), giving $J_1 = +101$, $J_2 = -45$, $J_3 = -9$ and $J_4 = -19$ cm^{-1} with $g = 1.94$. Data for **2** are shown in ESI† (Fig. S3), and give $J_1 = +118$, $J_2 = -49$, $J_3 = -6$ and $J_4 = -11$ cm^{-1} with $g = 1.87$.

$$H = -2J_1(\hat{S}_1\cdot\hat{S}_4 + \hat{S}_1\cdot\hat{S}_{4A} + \hat{S}_{1A}\cdot\hat{S}_4 + \hat{S}_{1A}\cdot\hat{S}_{4A}) - 2J_2\hat{S}_1\cdot\hat{S}_{1A} - 2J_3(\hat{S}_1\cdot\hat{S}_2 + \hat{S}_1\cdot\hat{S}_3 + \hat{S}_{1A}\cdot\hat{S}_{2A} + \hat{S}_{1A}\cdot\hat{S}_{3A}) - 2J_4(\hat{S}_2\cdot\hat{S}_3 + \hat{S}_{2A}\cdot\hat{S}_{3A}) \quad (1)$$

The high temperature part of the curve is sensitive to J_1 and J_2, and these parameters have to be strongly ferromagnetic and moderately antiferromagnetic, respectively. The low temperature region is more sensitive to J_3 and J_4 which have to be relatively weakly antiferromagnetic. These are the interactions within the oxo-centered triangles and their values are similar to those in, for example, $[V_3O(O_2CMe)_6(py)_3]ClO_4$.[9] We were unable to model the data with $J_3 = J_4$ or with $J_1 = J_3$. The latter is intruiging since the bridging is similar (two bta^- and an oxide) yet the J values are very different. Note that both involve the seven-coordinate, capped (O2) trigonal prismatic V1 ion. It may be that the ligand field splitting for this geometry[10] leads to different exchange pathways for V1···V4 and V1···V2/3. Testing this requires detailed electronic structure calculations which will be reported later.

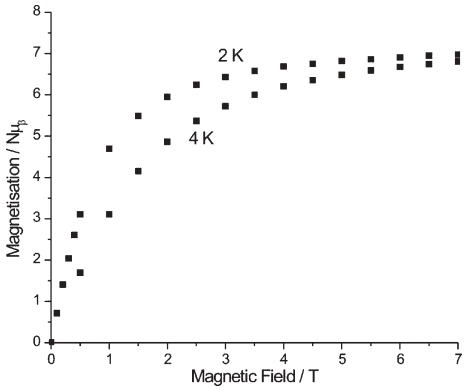

Fig. 3 M *vs.* H for **1** at 2 and 4 K.

J_1 and J_2 are the wingtip–body and body–body interactions, respectively, in the butterfly fragment. $[V_4O_2(O_2CEt)_7(bipy)_2]ClO_4$ is the only V^{III} butterfly reported to date,[7] where $J_1 = +28$ and $J_2 = -31$ cm^{-1}. These authors found by Kambé methods that the competing interactions stabilise an $S = 3$ state for $0.5 < |J_1/J_2| < 1.0$ (including their experimental data). For **1** (and **2**) we observe much (*ca.* four-fold) stronger ferromagnetic J_1. Given that J_4 acts to align both pairs of peripheral ions antiparallel, we expect an overall $S = 4$ ground state. Indeed, the eigenvalues of eqn (1) for compound **1** from matrix diagonalisation give $S = 4$ with a degenerate pair of $S = 3$ first excited states at 19 cm^{-1}, resulting from the relatively small and antiferromagnetic J_3 and J_4. Low-temperature magnetisation data as a function of applied field confirm the $S = 4$ ground state with a low g-value (Fig. 3).

W-Band (*ca.* 94 GHz) EPR spectra on polycrystalline samples of **1** and **2** are well resolved below *ca.* 30 K (Fig. 4 and 5). At 5 K, four intense regularly spaced transitions are observed to the low-field side of $g \approx 2.0$, with higher field transitions becoming observable at higher temperature. This is the $2S$ multiplet fine structure arising from the $S = 4$ ground state. Better resolution is observed for **2** (Fig. 5), where at 15 K we observe up to the seventh transition with the eighth lying at the 6 T field limit of our magnet.

Although these spectra appear to be of an axial $S = 4$ state dominated by the perpendicular transitions, it is not possible to simulate them on this basis. In fact, the spectra show characteristics of alignment of the crystallites in the large applied fields, thus implying significant magnetic anisotropy.[11] If the same

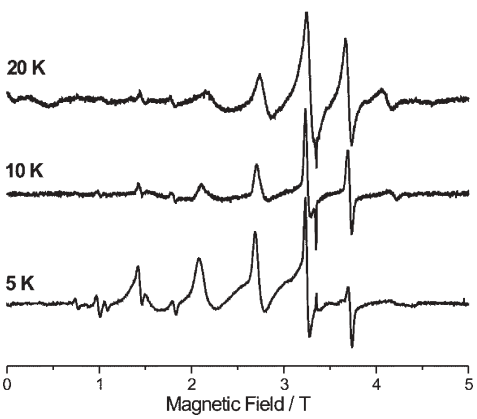

Fig. 4 W-Band EPR spectra of a loose polycrystalline sample of **1**.

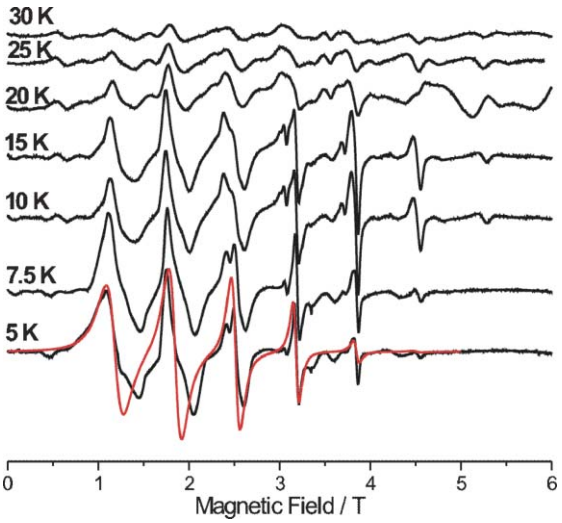

Fig. 5 W-Band EPR spectra of a loose polycrystalline sample of **2** (black), and simulation of the 5 K spectrum assuming a single orientation and the parameters in the text.

polycrystalline material is restrained in wax prior to exposure to the field, different (and complicated) spectra are observed which are not true powder spectra due to incomplete averaging (for example, see ESI,† Fig. S4 and S5; measured on a resonator-free high-frequency set-up allowing large amounts of sample). This is normally overcome by pressing or grinding the sample, but this leads to oxidation of **1** and **2** (even when performed in a glove box). **1** and **2** are not sufficiently soluble to measure frozen solution spectra.

However, the aligned spectra can be analysed to obtain the ground state D. Analysis of the crystal packing shows that in **2** the dianions are aligned while in **1** there are two distinct orientations. Therefore, in **2** the easy axis of magnetisation of the crystal, which will tend to align with the field, will be identical to that of the dianions. This is not the case in **1**. Hence, for **2** we can simulate the intense features assuming a single orientation with the field parallel to the principal axis of the **D** tensor (D_z), using $\mathrm{H} = g_z\mu_\beta \boldsymbol{B}\cdot\hat{S} + D[\hat{S}_z^2 - S(S+1)/3]$ with $S = 4$, $g_z = 1.91$ and $D = -0.297$ cm^{-1} (Fig. 5). Note this gives *no* information about the rhombic ZFS term, E. The Boltzmann effects can only be reproduced with a negative D.

Unfortunately, neither **1** nor **2** show M *vs.* H hysteresis loops (*e.g.* Fig. S6, ESI†) or out-of-phase ac susceptibility signals. Hence, they are not SMMs despite the large S and negative D. This is most likely because of a significant transverse anisotropy (E), which will require single-crystal EPR to determine. Nevertheless, we have demonstrated that very strong ferromagnetic $V^{III}\cdots V^{III}$ coupling, and significant magnetic anisotropy, can be built into high nuclearity and high spin ground state V^{III} clusters. Moreover, we have shown that $[V_2Cl_9]^{3-}$ is a promising starting material and we are actively investigating its use in cluster chemistry.

We thank the EPSRC and the EC ("Magmanet") for funding.

Notes and references

‡ Calc. (%) for **1**·3THF, $V_8O_{15}N_{26}Cl_6C_{112}H_{164}$: C 49.2, H 6.0, Cl 7.8, N 13.3, V 14.9. Found: C 50.1, H 5.1, Cl 7.6, N 14.3, V 15.1. Selected IR data (KBr): cm^{-1} 2960 (s), 2930 (s), 1572 (s), 1484 (s), 1428 (s), 1364 (m), 1380 (m), 1275 (m), 1231 (m), 1195 (s), 1064 (m), 998 (m), 792 (s), 700 (m), 671 (s), 649 (m), 564 (m), 532 (s), 451 (m), 440 (m). Calc. (%) for **2**·THF, $C_{112}H_{132}Cl_6N_{26}O_{13}V_8$: C 50.4, H 5.0, N 13.6, Cl 8.0, V 15.3. Found: C 50.1, H 5.1, N 14.3, Cl 7.6, V 15.1. **1** and **2** as solids degrade rapidly on exposure to air and all manipulations, in synthesis and for magnetic and spectroscopic studies, were conducted under an inert atmosphere.

§ *Crystal data* for **1**·4THF: $C_{116}H_{168}Cl_6N_{26}O_{16}V_8$, $M = 2802$, monoclinic, space group $P2_1/n$, $a = 14.4394(5)$, $b = 20.0945(7)$, $c = 22.9242(8)$ Å, $\beta = 96.395(3)^\circ$, $U = 6610.1(4)$ Å^3, $T = 100$ K, $Z = 2$, 43757 reflections collected, 11239 unique ($R_{int} = 0.0450$), $R(F) = 0.0593$ and $wR2 = 0.1470$ for $I > 2\sigma(I)$ [$R(F) = 0.0827$, $wR2 = 0.1593$ for all data]. *Crystal data* for **2**·2THF: $C_{116}H_{134}Cl_6N_{26}O_{14}V_8$, $M = 2737$, triclinic, space group $P\bar{1}$, $a = 13.2856(8)$, $b = 14.7996(7)$, $c = 18.4967(9)$ Å, $\alpha = 66.701(5)$, $\beta = 77.315(5)$, $\gamma = 80.523(5)^\circ$, $U = 3246.4(3)$ Å^3, $T = 100$ K, $Z = 1$, 19141 reflections collected, 9300 unique ($R_{int} = 0.0378$), $R(F) = 0.0862$ and $wR2 = 0.2469$ for $I > 2\sigma(I)$ [$R(F) = 0.0778$, $wR2 = 0.2254$ for all data]. CCDC 654038 and 654039. For crystallographic data in CIF or other electronic format see DOI: 10.1039/b710732c

¶ Magnetic data were measured (0.1–1 T applied fields for $\chi(T)$ measurements) using a Quantum Design XL7 SQUID magnetometer, and were corrected for diamagnetic contributions according to Pascal's tables; very low temperature measurements used a micro-SQUID array.[12] Data were fitted using MAGPACK.[13] W-Band EPR spectra were measured on a Bruker E600 CW spectrometer; 190 and 270 GHz spectra were recorded on home-built apparatus.[14] Simulations used Weihe's SimEPR.[15]

1 For a recent review, see: G. Aromí and E. K. Brechin, *Struct. Bonding*, 2006, **122**, 1.
2 J. Krzystek, A. T. Fiedler, J. J. Sokol, A. Ozarowski, S. A. Zvyagin, T. C. Brunold, J. R. Long and J. Telser, *Inorg. Chem.*, 2004, **43**, 5645.
3 P. Knopp, K. Weighardt, B. Nuber, J. Weiss and W. S. Sheldrick, *Inorg. Chem.*, 1990, **29**, 363; S. G. Brand, N. Edelstein, C. J. Hawkins, G. Shalimoff, M. R. Snow and E. R. T. Tiekink, *Inorg. Chem.*, 1990, **29**, 434.
4 (*a*) R. H. Laye, M. Murrie, S. Ochsenbein, A. R. Bell, S. Teat, J. Raftery, H. U. Güdel and E. J. L. McInnes, *Chem.–Eur. J.*, 2003, **9**, 6215; (*b*) S. Khanra, M. Kloth, H. Mansaray, C. A. Muryn, F. Tuna, E. C. Sañudo, M. Helliwell, E. J. L. McInnes and R. E. P. Winpenny, *Angew. Chem., Int. Ed.*, 2007, **46**, 5568.
5 R. Shaw, R. H. Laye, L. F. Jones, D. M. Low, C. Talbot-Eeckelaers, Q. Wei, C. J. Milios, S. Teat, M. Helliwell, J. Raftery, M. Evangelisti, M. Affronte, D. Collison, E. K. Brechin and E. J. L. McInnes, *Inorg. Chem.*, 2007, **46**, 4968; I. S. Tidmarsh, R. H. Laye, P. R. Brearley, M. Shanmugam, E. C. Sañudo, L. Sorace, A. Caneschi and E. J. L. McInnes, *Chem.–Eur. J.*, 2007, **13**, 6329.
6 H. Kumagai and S. Kitagawa, *Chem. Lett.*, 1996, 471.
7 S. L. Castro, Z. Sun, C. M. Grant, J. C. Bollinger, D. N. Hendrickson and G. Christou, *J. Am. Chem. Soc.*, 1998, **120**, 2365.
8 G. B. Karet, S. L. Castro, K. Folting, J. C. Bollinger, R. A. Heintz and G. Christou, *J. Chem. Soc., Dalton Trans.*, 1998, 67.
9 S. L. Castro, W. E. Streib, J.-S. Sun and G. Christou, *Inorg. Chem.*, 1996, **35**, 4462.
10 R. Hoffmann, B. F. Beier, E. L. Muetterties and A. R. Rossi, *Inorg. Chem.*, 1977, **16**, 511.
11 A.-L. Barra, L.-C. Brunel, D. Gatteschi, L. Pardi and R. Sessoli, *Acc. Chem. Res.*, 1998, **31**, 460.
12 W. Wernsdorfer, *Adv. Chem. Phys.*, 2001, **118**, 99.
13 J. J. Borrás-Almenar, J. M. Clemente-Juan, E. Coronado and B. S. Tsukerblat, *J. Comput. Chem.*, 2001, **22**, 985.
14 F. Muller, M. A. Hopkins, N. Coron, M. Grynberg, L.-C. Brunel and G. Martinez, *Rev. Sci. Instrum.*, 1989, **60**, 3681.
15 C. H. J. Jacobsen, E. Pederson, J. Villadsen and H. Weihe, *Inorg. Chem.*, 1993, **32**, 1216.